

The crystal structure and thermal expansion of the perovskite-type $\text{Nd}_{0.75}\text{Sm}_{0.25}\text{GaO}_3$: powder diffraction and lattice dynamical studies

A Senyshyn¹, A R Oganov², L Vasylechko¹, H Ehrenberg³, U Bismayer⁴, M Berkowski⁵ and A Matkovskii^{1,6}

¹ Lviv Polytechnic National University, Bandera Street 12, 79013 Lviv, Ukraine

² Laboratory of Crystallography, Department of Materials, ETH Zurich, CH-8092 Zurich, Switzerland

³ Darmstadt University of Technology, Institute for Materials Science, Petersenstrasse 23, D-64287 Darmstadt, Germany

⁴ Mineralogisch-Petrographisches Institut, Universität Hamburg, Grindelallee 48, D-20146 Hamburg, Germany

⁵ Institute of Physics Polish Academy of Sciences, Al. Lotników 32/46, 02-668 Warsaw, Poland

⁶ Institute of Physics, Rzeszów University, Rejtana 16A, 35-310 Rzeszów, Poland

Received 25 September 2003

Published 9 January 2004

Online at stacks.iop.org/JPhysCM/16/253 (DOI: 10.1088/0953-8984/16/3/006)

Abstract

The structure of $\text{Nd}_{0.75}\text{Sm}_{0.25}\text{GaO}_3$ was studied by high-resolution powder diffraction methods using conventional x-ray and synchrotron radiation in the temperature range 85–1173 K. The GdFeO_3 structure type was confirmed for $\text{Nd}_{0.75}\text{Sm}_{0.25}\text{GaO}_3$ in the temperature region investigated and no structural transitions were observed. The cell parameters show a monotonic and anisotropic increase with temperature. The interatomic potential was fitted using the GULP code. Using this potential, a self-consistent approximation following the Debye model was constructed from the elastic constants of the crystals. The total phonon DOS, its projections onto atomic species, heat capacity C_v , Grüneisen parameter γ and thermal expansion coefficient α were considered in the framework of quasiharmonic lattice dynamics and the Debye model. The shape of the phonon DOS calculated from lattice dynamics differs significantly from the respected Debye DOS. The rare earth, gallium and oxygen atoms dominate in different frequency regions of the phonon spectrum. The heat capacity is well reproduced by the Debye model below 100 K, where acoustic phonons play an important role and above 800 K when the classical limit is reached. Predicted values of Grüneisen parameter and thermal expansion coefficients in the frame of the Debye model are $\sim 35\%$ too low. Therefore, the thermal properties of $\text{Nd}_{0.75}\text{Sm}_{0.25}\text{GaO}_3$ cannot be explained by acoustic phonons only and hence, $\text{Nd}_{0.75}\text{Sm}_{0.25}\text{GaO}_3$ cannot be described perfectly as a Debye-like solid with respect to its thermodynamic properties.

(Some figures in this article are in colour only in the electronic version)

1. Introduction

In recent years rare-earth perovskite-type orthogallates REGaO_3 (RE—rare-earth ion) have been studied intensively because of their wide range of unique physical properties. Most well-known applications are for substrate materials for HTSC and CMR films [1, 2]. For example, NdGaO_3 single crystals are a promising substrate material for GaN film deposition [3], and Sr- and Mg-doped LaGaO_3 is a prospective material for fuel cells [4]. Also, ionic conductivity has been reported for doped NdGaO_3 [5] and PrGaO_3 [6, 7].

From the family of rare-earth perovskite-type orthogallates, the NdGaO_3 – SmGaO_3 pseudo-binary system is unique from the technological point of view. As reported in [8–11], rare-earth orthogallates REGaO_3 with RE ionic radii smaller than the neodymium radius (RE = Sm–Lu) cannot be obtained by solid-phase synthesis methods. In the literature, two well established methods for obtaining such compounds have been described: either by the decomposition of the corresponding garnet phases at high temperatures and pressures (45 kbar, 1000 °C) using a NaOH melt, or by overheating of a $0.5 \text{ RE}_2\text{O}_3$ – $0.5 \text{ Ga}_2\text{O}_3$ (RE = Sm–Er) melt [11].

The growth of $\text{Nd}_{1-x}\text{Sm}_x\text{GaO}_3$ crystals ($x = 0.25, 0.50, 0.75, 0.9$) has been reported by Aleksiyko *et al* [12]. They found the smallest cell volume for $\text{Nd}_{0.25}\text{Sm}_{0.75}\text{GaO}_3$ within the whole rare-earth orthogallates family and concluded that $\text{Nd}_{1-x}\text{Sm}_x\text{GaO}_3$ samples with Nd substitution by Sm atoms higher than 75 mol% cannot be synthesized at ambient pressure. In [13] the synthesis of a sample with 57 wt% of SmGaO_3 in the perovskite phase and GdFeO_3 -type of structure at RT has been presented. The authors of [13] concluded that the existence of continuous solid solutions in the NdGaO_3 – SmGaO_3 pseudo-binary system is limited by the Sm content of 75–80 mol%. Structure investigations of $\text{Nd}_{1-x}\text{Sm}_x\text{GaO}_3$ ($x = 0.25, 0.50$) at RT were also reported in [13], and for all studied samples an orthorhombically distorted GdFeO_3 -type of structure ($Pbnm$ space group) was found.

The space group $Pbnm$ occurs frequently in the large family of perovskites. According to [14] the $Pbnm$ space group covers more than 60% of all known compounds with perovskite-type structure. This symmetry is preserved even under extreme conditions (for example, MgSiO_3 perovskite is the major mineral of the Earth's lower mantle [15]) for systems with a high Goldschmidt tolerance factor.

The fact that rare-earth perovskite-type orthogallates are most suitable as substrate materials in HTSC devices or as interconnecting material in solid oxide fuel cells (SOFC), operating at 77 and 700 K, respectively, makes the thermal behaviour of these structures a highly important research object.

In this work the structure of $\text{Nd}_{0.75}\text{Sm}_{0.25}\text{GaO}_3$ has been studied in detail by high-resolution powder diffraction using conventional x-ray and synchrotron radiation in the temperature range 85–1173 K. Taking into account the different atomic masses of the constituent components, the system attracts the attention for simulations by lattice dynamics. Therefore, calculations based on the Debye model are compared with quasiharmonic lattice dynamics.

2. Experimental details

The $\text{Nd}_{0.75}\text{Sm}_{0.25}\text{GaO}_3$ sample for our investigations was grown by the Czochralski technique [12]. The crystal structure of $\text{Nd}_{0.75}\text{Sm}_{0.25}\text{GaO}_3$ and its thermal evolution in the temperature range 85–1173 K was studied using the high-resolution powder diffraction technique. Low-temperature (LT) structural investigations in the temperature range 85–320 K were performed on a STOE powder diffractometer equipped with a liquid nitrogen coldfinger from Oxford Cryosystems using $\text{Mo K}\alpha_1$ -radiation. Diffraction patterns were collected in the

Table 1. The structural parameters of Nd_{0.75}Sm_{0.25}GaO₃ at different temperatures as refined from high-resolution powder diffraction data. The space group is *Pbnm* (No 62). The numbers in parentheses give statistical errors in the last significant digit.

	85 K	RT	1173 K
<i>a</i> (Å)	5.4046(2)	5.412 56(3)	5.469 18(5)
<i>b</i> (Å)	5.4971(2)	5.499 62(3)	5.525 93(6)
<i>c</i> (Å)	7.6779(3)	7.690 63(4)	7.769 15(8)
<i>V</i> (Å ³)	228.11(2)	228.927(4)	234.802(7)
Nd/Sm, 4c			
<i>x</i>	−0.0099(5)	−0.0109(2)	−0.0079(6)
<i>y</i>	0.0458(3)	0.0440(1)	0.0362(2)
<i>z</i>	$\frac{1}{4}$	$\frac{1}{4}$	$\frac{1}{4}$
<i>B</i> (is/eq)	0.27(3)	0.56(1)	1.19(2)
Ga, 4b			
<i>x</i>	$\frac{1}{2}$	$\frac{1}{2}$	$\frac{1}{2}$
<i>y</i>	0	0	0
<i>z</i>	0	0	0
<i>B</i> (is/eq)	0.47(7)	0.49(2)	0.55(4)
O1, 4c			
<i>x</i>	0.085(5)	0.088(2)	0.085(3)
<i>y</i>	0.488(4)	0.478(2)	0.482(3)
<i>z</i>	$\frac{1}{4}$	$\frac{1}{4}$	$\frac{1}{4}$
<i>B</i> (is/eq)	0.6(5)	1.8(2)	3.3(5)
O2, 8d			
<i>x</i>	−0.289(4)	−0.296(2)	−0.291(2)
<i>y</i>	0.295(3)	0.287(2)	0.295(2)
<i>z</i>	0.045(3)	0.0433(11)	0.040(2)
<i>B</i> (is/eq)	0.2(3)	1.5(2)	1.0(3)
<i>R_I</i>	0.0678	0.0582	0.0705
<i>R_P</i>	0.1671	0.1361	0.1760

2θ -range from 8° to 56° with a step size of 0.02° at temperatures of 85, 110, 140, 170, 200, 230, 260, 290 and 320 K. For high-temperature (HT) structural investigations the synchrotron powder diffractometer at beamline B2, HASYLAB, DESY, Hamburg, Germany, was used. The wavelength was selected close to the Mo $K\alpha_1$ wavelength and was determined to be 0.708 79(5) Å based on five reflections of a Si NBS640b standard. Full patterns were collected using the on-site readable image plate detector OBI [16] over the 2θ -range 7.48°–85° with a step size 0.004° at RT, 373, 473, 573, 673, 773, 873, 973, 1073 and 1173 K. All measurements were performed in Debye–Scherrer mode. Analysis of the data was carried out using the WinCSD program package [17].

3. Results and discussion

3.1. Crystal structure

At RT Nd_{0.75}Sm_{0.25}GaO₃ adopts the orthorhombically distorted GdFeO₃-type structure in agreement with [13]. This type of structure is confirmed for all temperatures investigated. Some characteristic results of Rietveld refinements for Nd_{0.75}Sm_{0.25}GaO₃ at 85 K, RT and 1173 K are presented in figure 1; the corresponding structure parameters are summarized in table 1. Projections of the Nd_{0.75}Sm_{0.25}GaO₃ structure along [001] and [100] directions are shown in figure 2.

The thermal evolution of the lattice parameters in the temperature range 85–1173 K is shown in figure 3. The lattice parameters of Nd_{0.75}Sm_{0.25}GaO₃ increase anisotropically and

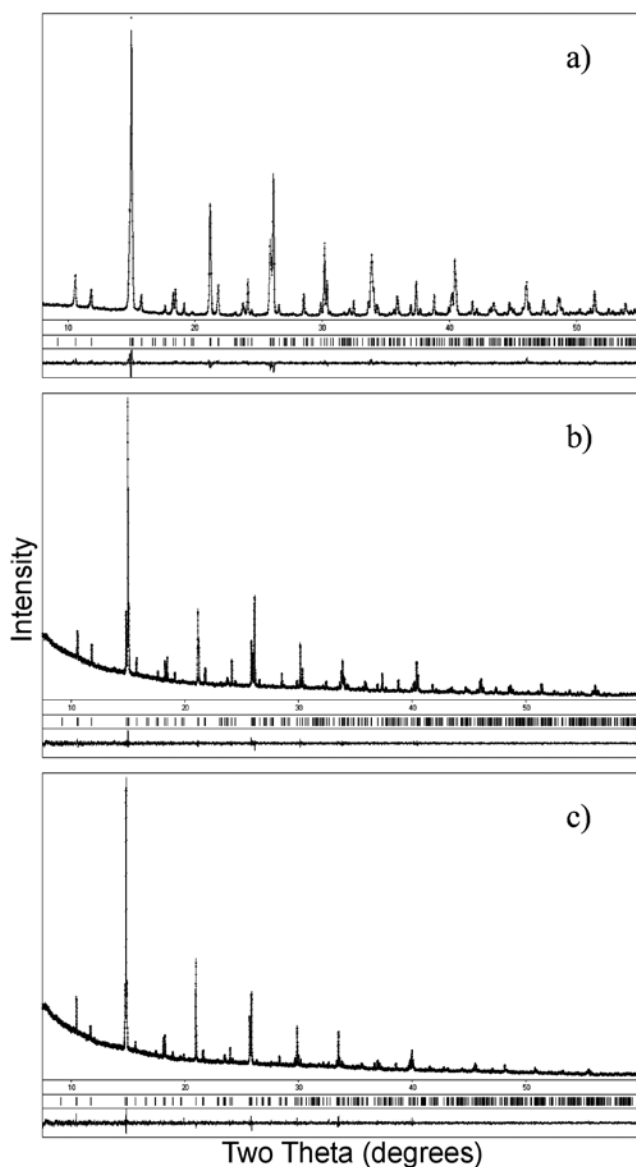


Figure 1. The graphical result of the Rietveld refinement for $\text{Nd}_{0.75}\text{Sm}_{0.25}\text{GaO}_3$ at 85 K (a) ($\text{Mo K}\alpha_1$ -radiation), at RT (b) and at 1173 K (c) ((b), (c) are synchrotron data, $\lambda = 0.70879(5) \text{ \AA}$).

nonlinearly with temperature. All data points were fitted by a polynomial of temperature of fourth order with the linear coefficient fixed to zero. The coefficients are given in table 2.

3.2. Lattice dynamics

For ionic materials, interatomic potentials in the form of a Buckingham potential is a rather traditional model, which has been shown to perform sufficiently well and, therefore, it is widely

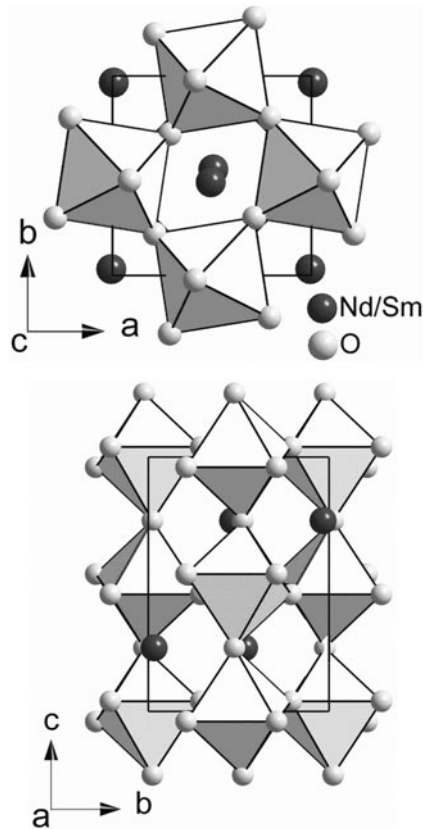


Figure 2. The structure of Nd_{0.75}Sm_{0.25}GaO₃ at RT as a framework of corner-sharing GaO₆ octahedra.

Table 2. The results of the polynomial fitting of the lattice parameters.

	a (Å)	b (Å)	c (Å)
a_0	5.4040(2)	5.4964(2)	7.673 83(25)
$a_1 \times 10^7$	1.26(4)	0.48(4)	0.87(6)
$a_2 \times 10^{10}$	-1.14(8)	-0.36(8)	-0.70(12)
$a_3 \times 10^{14}$	4.0(4)	1.2(4)	2.3(6)
R (COD)	0.999 79	0.998 98	0.999 80

used for modelling various oxides. This potential takes the form

$$U_{ij}(r_{ij}) = \frac{Z_i Z_j}{r_{ij}} + b_{ij} \exp\left(-\frac{r_{ij}}{\rho_{ij}}\right) - \frac{c_{ij}}{R_{ij}^6} \quad (1)$$

where the individual terms represent the Coulomb potential, Born–Mayer repulsion and van der Waals energies, respectively. Here r_{ij} is the interatomic distance between atoms i and j , Z_i is the effective charge of the i th atom, b_{ij} , ρ_{ij} and c_{ij} are the short-range potential parameters for each pair of atoms usually found by fitting to experimental data [18–21]. Unfortunately, a potential based on parameters presented by latter authors does not reproduce

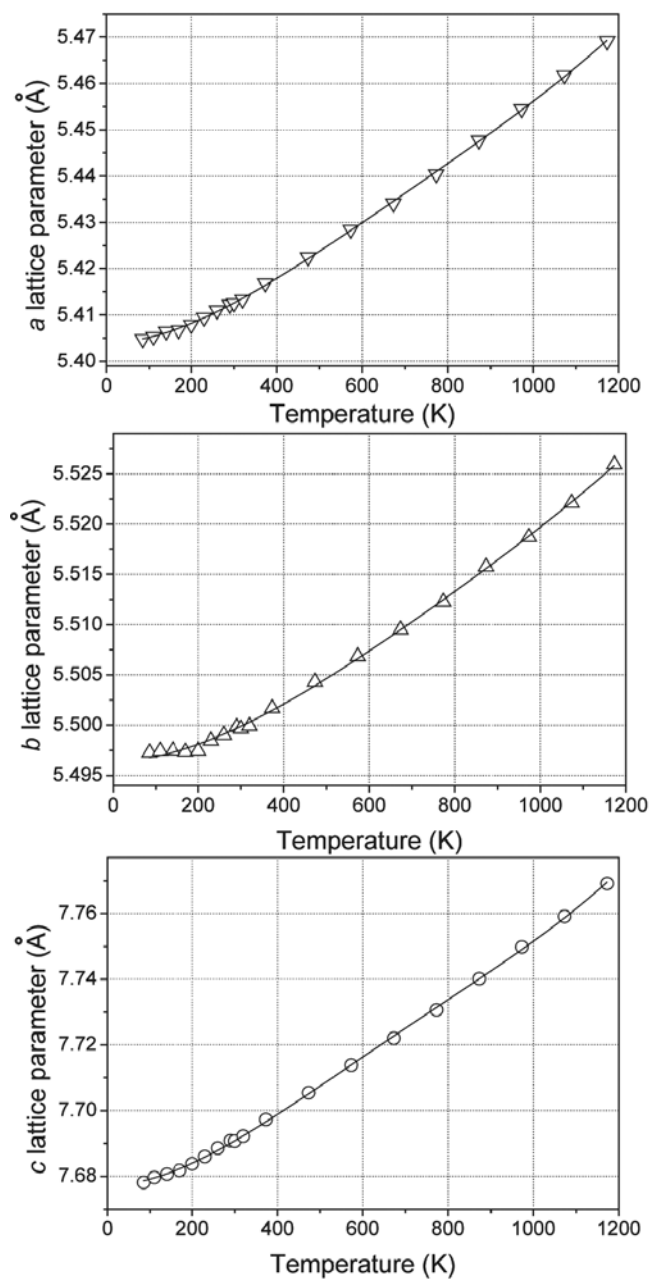


Figure 3. Thermal evolution of the orthorhombic lattice parameters (the solid curve is the polynomial fit).

the $\text{Nd}_{0.75}\text{Sm}_{0.25}\text{GaO}_3$ structure accurately and, therefore, a different approach was developed to reproduce the properties of $\text{Nd}_{0.75}\text{Sm}_{0.25}\text{GaO}_3$ with a reasonable precision. For the potentials described, O–O short-range interactions were chosen from [18], which were successfully used for the modelling of perovskite-type oxides. We neglected the van der Waals interactions for

Table 3. The parameters of the potential (equation (1)).

Short-range interaction			
Interaction	b_{ij} (eV)	ρ (eV Å)	c (Å ⁶)
Nd ³⁺ -O ²⁻	2 686.6	0.320 6	0.0
Sm ³⁺ -O ²⁻	4 040.9	0.303 4	0.0
Ga ³⁺ -O ²⁻	513.4	0.387 0	0.0
O ²⁻ -O ²⁻	22 764.0	0.149 00	27.879
Shell model ^a			
Ion	$Y(e)$	k (eV Å ⁻²)	
O ²⁻	-2.869 02	74.92	

^a Y and k refer to the shell charge and harmonic spring constant respectively.

Table 4. Selected experimental and calculated structure properties of Nd_{0.75}Sm_{0.25}GaO₃.

	Experimental	Calculated	
V (Å ³)	228.11	226.42	
a (Å)	5.4046	5.4246	
b (Å)	5.4971	5.4694	
c (Å)	7.6779	7.6316	
Nd/Sm, 4c	x	0.9901	0.9967
	y	0.0458	0.0274
O1, 4c	x	0.0850	0.0623
	y	0.4880	0.4804
O2, 8d	x	0.7110	0.7128
	y	0.2950	0.2876
	z	0.0450	0.0327

cation–anion interactions because this type of interaction is significant only between large and polarizable atoms or ions.

The crystal structures of Nd_{0.75}Sm_{0.25}GaO₃, Nd_{0.50}Sm_{0.50}GaO₃ [13], NdGaO₃ [22], Ga₂O₃, and Sm₂O₃ [23] at 300 K were fitted simultaneously using the GULP [24] code. The best agreement was obtained with the parameters listed in table 3. Some results of the fit are listed in table 4 along with the experimental data.

Our lattice dynamics calculations were also performed using GULP. For the minimization of the free energy, calculations of the density of states (DOS) and its projections, and the heat capacity (C_v), a $20 \times 20 \times 20$ Monkhorst–Pack grid was used for the Brillouin zone integration. The free energy minimization was performed without the zero static internal stress approximation and showed good convergence. The vibrational DOS and its projections onto atomic contributions are calculated using the interatomic potential from equation (1) with parameters displayed in table 3, and are shown in figure 4 in comparison with the Debye DOS $g(\omega)$

$$g(\omega) = \begin{cases} 9n \left(\frac{h}{k_B \theta_D} \right)^2 \omega^2, & \omega \leq \frac{k_B \theta_D}{h}, \\ 0, & \omega > \frac{k_B \theta_D}{h}, \end{cases} \quad (2)$$

where n is the number of atoms in the cell, ω is the frequency, k_B is Boltzmann's constant, and h is Planck's constant. The Debye temperature θ_D is calculated from the elastic constants

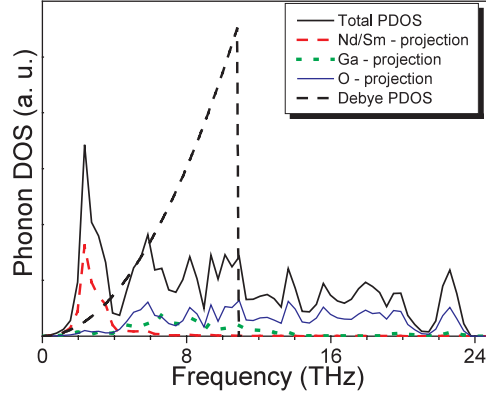


Figure 4. The calculated density of states of $\text{Nd}_{0.75}\text{Sm}_{0.25}\text{GaO}_3$.

using the relation

$$\theta_D = \frac{\hbar}{k_B} \left(\frac{6\pi^2}{V_{\text{at}}} \right)^{1/3} \left[\frac{1}{3} \left(\frac{3K + 4G}{3\rho} \right)^{-3/2} + \frac{2}{3} \left(\frac{G}{\rho} \right)^{-3/2} \right]. \quad (3)$$

V_{at} is the volume per atom, ρ is the density, and K and G are the bulk and shear modulus, respectively. The Debye temperature was calculated from the full elastic constant tensor averaged by the Reuss–Voigt–Hill scheme ($K = 192.6$ GPa, $G = 99.2$ GPa) using equation (3). Accordingly, the calculated Debye temperature for $\text{Nd}_{0.75}\text{Sm}_{0.25}\text{GaO}_3$ is 528 K. Taking into account the substitution of 25% Nd by Sm atoms, the obtained results correlate well with the data obtained by Krivchikov *et al* [25], where the Debye temperature and elastic constants were obtained from ultrasound velocities in pure NdGaO_3 ($K = 190.0$ GPa, $G = 92.4$ GPa, $\theta_D = 513$ K).

In figure 4 the DOS, projections of the DOS onto the atomic species from phonon calculations, and the Debye DOS are presented. The shape of the full-phonon DOS differs significantly from the Debye DOS. Moreover, projections of the DOS show significant deviations from the ‘acoustic’ behaviour. For a Debye-type behaviour all atoms contribute at each frequency to a constant proportion of the total DOS, determined by relative masses and numbers of atoms of each sort. Full phonon calculations show a slightly different behaviour: the rare-earth ion dominates in the low-frequency branches, Ga shows the maximum of its influence in the intermediate region of the phonon spectrum, whereas oxygen tends to contribute in the intermediate- and high-frequency region of the DOS. The contributions to frequency ranges result from significant differences in atomic weights. A similar situation has been observed in other rare-earth perovskites.

Anderson *et al* [26] formulated the following preconditions to derive a reasonable $C_v(T)$ from the Debye approximated DOS:

- (a) no gaps should occur in the phonon spectrum;
- (b) not many modes should have frequencies above the maximum Debye frequency;
- (c) the phonon density of states should be close to equation (4) at least in the limit of small ω .

As shown in figure 4, none of the criteria formulated by Anderson is fully satisfied for the observed DOS and, therefore, no reliable calculation of the harmonic properties, in particular of the specific heat capacity, is expected within the framework of the Debye model.

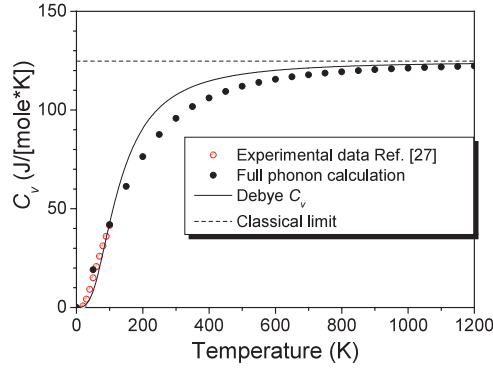


Figure 5. The heat capacity at constant volume as a function of temperature.

From the harmonic approximation, all thermodynamic properties can be calculated by integration over all frequencies

$$C_v(T) = k_B \int g(\omega) \left(\frac{\hbar\omega}{k_B T} \right)^2 \frac{\exp\left(\frac{\hbar\omega}{k_B T}\right)}{\left(\exp\left(\frac{\hbar\omega}{k_B T}\right) - 1\right)^2} d\omega, \quad (4)$$

where $g(\omega)$ is the total phonon DOS from the full-phonon calculations. The Debye model gives the following expression for C_v :

$$C_v(T) = 3k_B n \left(12 \left(\frac{T}{\theta_D} \right)^3 \int_0^{\theta_D/T} \frac{x^3}{e^x - 1} dx - \frac{3\theta_D/T}{\exp(\theta_D/T) - 1} \right). \quad (5)$$

In figure 5, the heat capacity at constant volume is presented as obtained from full-phonon calculations, and in the framework of the Debye model (by equations (4) and (5), respectively). Both the Debye model and the full-phonon calculations result in very similar $C_v(T)$ at LT (below 100 K), whereas at higher temperatures up to 800 K, when the classical limit is reached, the differences are more pronounced. In [27] the lattice heat capacity, calculated from the observed heat capacity for pure NdGaO₃, was reported. These results are presented in figure 5 by open points, and indicate good agreement between the experimental heat capacity and the calculated ones.

In recent years, the fitting of experimental results by different Debye functions (e.g. heat capacity [27], internal energy [28, 29] and thermal expansion [30, 31]) has been applied for different perovskite-type oxides with the aim of estimating the Debye temperature and related properties. In this work the Debye temperature is determined by fitting the Debye C_v to the data obtained from full-phonon calculations (results obtained from equation (4) were fitted by equation (5)). The Debye temperature was the only fitted parameter, and it converged to 632 K for Nd_{0.75}Sm_{0.25}GaO₃, which is in good agreement with the reported value $\theta_D = 676$ K, obtained for pure NdGaO₃ [27].

The results demonstrate the explanation of the experimental heat capacity even by crude approximations. Nevertheless, the differences between Debye temperatures, on the one hand calculated from elastic constants and on the other hand fitted to the experimental heat capacity curves, indicate the insufficiency of the Debye model for the precise description of thermodynamic functions in the case of perovskite-like rare-earth orthogallates and their solid solutions.

The Grüneisen parameter was calculated using the quasiharmonic formula,

$$\gamma_{TH} = \frac{\sum_{i,k} C_{i,k} \gamma_{i,k}}{\sum_{i,k} C_{i,k}}. \quad (6)$$

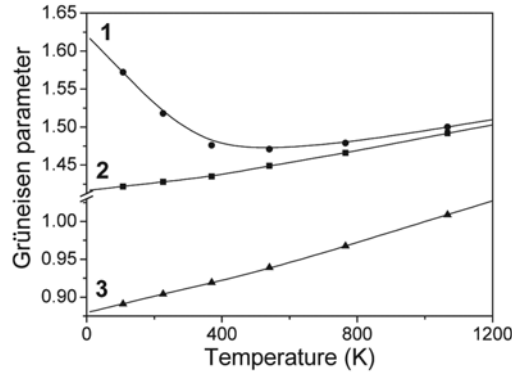


Figure 6. The Grüneisen parameter versus temperature (the curves are guides for the eye).

where $C_{i,k}$ is the partial heat capacity of all phonon modes at the k -points of the Brillouin zone. In the high-temperature limit, equation (6) reduces to the arithmetic mean of the i th mode Grüneisen parameter $\gamma_{i,k}$,

$$\gamma_{\text{TH}} = \langle \gamma_{i,k} \rangle. \quad (7)$$

Within the Debye model, the Grüneisen parameter can be calculated using the quasiharmonic relation

$$\gamma = - \frac{d \ln \theta_D}{d \ln V}. \quad (8)$$

Curve 1 in figure 6 represents the Grüneisen parameter as calculated using equation (6). The Grüneisen parameter decreases on heating in the low-temperature region and has a minimum at ~ 530 K (which might correlate with the Debye temperature). With further increasing temperature, the Grüneisen parameter increases and shows ‘classical’ behaviour above 800 K (curve 2, calculated via equation (7)). The ‘acoustic’ Grüneisen parameter is underestimated in the Debye model (curve 3 calculated by equation (8)) compared with the Grüneisen parameter calculated from the full-phonon calculations, because only acoustic phonons are taken into account in the Debye model, which are of primary importance only at LT. The low values for the ‘acoustic’ Grüneisen parameter are probably the reason for the large deviations between the observed and the Debye-model thermal expansion coefficients calculated following the Grüneisen law

$$\alpha = \frac{\gamma \rho C_v}{K_T}. \quad (9)$$

The thermal expansion was calculated based on the results of full-phonon calculations (curve 1 in figure 7) and within the Debye model approximations (curve 2 in figure 7), where the respective values of γ and C_v were used. As seen in figure 7, the ‘acoustic’ Grüneisen parameter given by the Debye model yields satisfying agreement at LT, whereas at higher temperatures the restriction to acoustic phonons leads to serious deviations in the thermal expansion.

Figure 8 illustrates the experimentally observed cell volume thermal evolution (squares) and cell volumes calculated from the thermal expansion coefficient according to Zhao [32] with

$$V(T) = V(T_0) \left(1 + \int_{T_0}^T \alpha(x) dx \right). \quad (10)$$

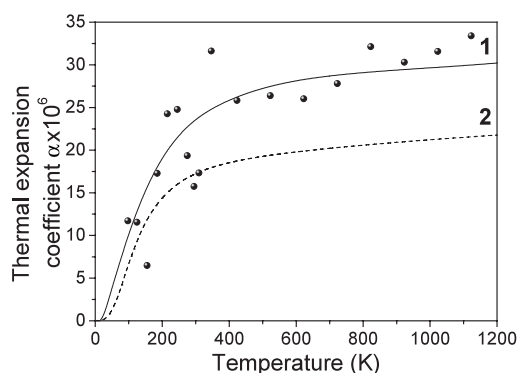


Figure 7. Volumetric thermal expansion coefficients versus temperature.

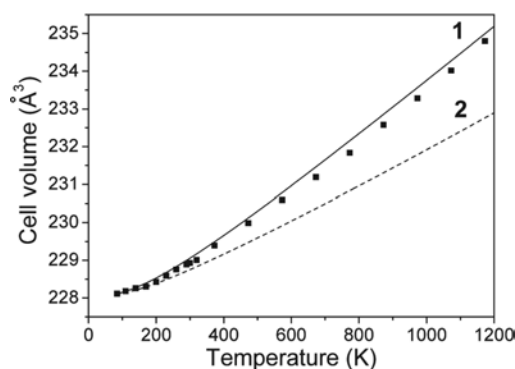


Figure 8. Cell volume thermal dependencies.

Curve 1 in figure 8 shows the cell volumes calculated using full-phonon calculations. Curve 2 in figure 8 is the results from the Debye model. Figure 8 shows the experimentally observed cell volumes, which are in good agreement with the full-phonon calculations while the Debye model results in 35% smaller expansion.

4. Conclusions

The structure of $\text{Nd}_{0.75}\text{Sm}_{0.25}\text{GaO}_3$ was studied by x -ray powder diffraction and synchrotron radiation in the temperature range 85–1173 K. The GdFeO_3 -type of structure was confirmed for the whole temperature region investigated. The cell parameters show a monotonic and anisotropic increase with temperature.

The thermal expansion of $\text{Nd}_{0.75}\text{Sm}_{0.25}\text{GaO}_3$ has been calculated by quasiharmonic lattice dynamics and using the Debye model. The interatomic potential used was presented by a combination of Coulomb potentials, Born–Mayer repulsion and van der Waals interactions. For better describing the Nd–O and Ga–O interactions, the crystal structures of $\text{Nd}_{0.75}\text{Sm}_{0.25}\text{GaO}_3$, $\text{Nd}_{0.50}\text{Sm}_{0.50}\text{GaO}_3$, NdGaO_3 , Ga_2O_3 , Nd_2O_3 , and Sm_2O_3 were fitted simultaneously using the GULP code.

In spite of this rather simple model, a good description of interatomic interactions was obtained by quasiharmonic lattice dynamics as indicated by the good agreement between observed and calculated thermal expansion and heat capacity.

We considered the total phonon DOS, projections onto atomic species, the heat capacity C_v , the Grüneisen parameter γ , and the thermal expansion coefficient α in the framework of quasiharmonic lattice dynamics and the Debye model. Comparing the total DOS and its projections with the Debye DOS, $\text{Nd}_{0.75}\text{Sm}_{0.25}\text{GaO}_3$ cannot be considered as a good Debye-like solid. The heat capacity is only well reproduced by the Debye model below 100 K, where acoustic phonons are playing an important role and above 800 K, i.e. close to the classical limit. The Grüneisen parameter and thermal expansion coefficient are calculated to be about 35% lower than experimentally observed. Therefore, the Debye model is not an appropriate description for the thermal behaviour of the $\text{Nd}_{0.75}\text{Sm}_{0.25}\text{GaO}_3$ structure. A similar conclusion has been reached for MgSiO_3 perovskite.

Acknowledgments

This work was supported by WTZ (UKR 01/12), Ukrainian Ministry of Science (Project No 2M/50-2000), the Polish Committee for Scientific Research (Grant N 7 T08A 00520) and ICDD Grant-in-aid program. AS gratefully acknowledges financial support from the *Deutscher Akademischer Austauschdienst (Leonhard–Euler program)*. LV acknowledges a research fellowship of the Max-Planck Society. We would like to thank Professor Julian D Gale for providing the GULP code and for helping us in using it.

References

- [1] Mogro-Campero A, Turner L G, Hall E L, Garbaskas M I and Lewis N 1989 *Appl. Phys. Lett.* **54** 2719
- [2] Sandstrom R L, Giess E A, Gallagher W J, Segmuller A, Cooper E I, Chisholm M F, Gupta A, Shinole S and Laibowitz R B 1988 *Appl. Phys. Lett.* **53** 1874
- [3] Mamutin V V, Toropov A A, Kartenko N F, Ivanov S V, Wagner A and Monemar B 1999 *Mater. Sci. Eng. B* **59** 56
- [4] Feng M and Goodenough J B 1994 *Eur. J. Solid. State Inorg. Chem.* **31** 663
- [5] Petric A and Huang P 1996 *Solid State Ion.* **92** 113
- [6] Liu Zh, Cong L, Huang X, Lu Zh and Su W 2001 *J. Alloys Compounds* **314** 281
- [7] Ishibara T, Furutani H, Arikawas H, Honda M, Akbay T and Takita Yu 1999 *J. Electrochem. Soc.* **146** 643
- [8] Schneider S J, Roth R S and Waring J L 1961 *J. Res. Nat. Bur. Stand.* **65** A345
- [9] Nicolas J, Coutures J, Coutures J P and Boudot B 1984 *J. Solid State Chem.* **52** 101
- [10] Marezio A, Remeika J P and Dernier P D 1968 *Inorg. Chem.* **7** 1337
- [11] Geller S, Curlander P J and Ruse G F 1974 *Mater. Res. Bull.* **9** 637
- [12] Aleksiyko R, Berkowski M, Byszewski P, Dabrowski B, Diduszko R, Fink-Finowicki J and Vasylechko L O 2001 *Cryst. Res. Technol.* **36** 789
- [13] Vasylechko L, Red'ko N, Fadeev S and Berkowski M 2001 *Visnyk Lviv Polytech.* **455** 21
- [14] Lufaso M W and Woodward P M 2001 *Acta Crystallogr. B* **57** 725
- [15] Oganov A R, Brodholt J P and Price G D 2001 *Nature* **411** 934
- [16] Knapp M, Joco V, Bächtz C, Brecht H H, Berghaeuser A, Ehrenberg H, von Seggern H and Fuess H 2003 *Nucl. Instrum. Methods A* at press
- [17] Akselrud L G, Zavalij P Yu, Grin Yu, Pecharsky V K, Baumgartner B and Woelfel E 1993 *Mater. Sci. Forum* **335** 133
- [18] Lewis G V and Catlow C R A 1985 *J. Phys. C: Solid State Phys.* **18** 1149
- [19] Bush T S, Gale J D, Catlow C R A and Battle P D 1994 *J. Mater. Chem.* **4** 831
- [20] Gale J D 1996 *Phil. Mag.* **B 73** 3
- [21] Islam M S, Cherry M and Catlow C R A 1996 *J. Solid State Chem.* **124** 230
- [22] Savvitskii D, Vasylechko L, Senyshyn A, Matkovskii A, Bächtz C, Sanjuán M L, Bismayer U and Berkowski M 2003 *Phys. Rev. B* **68** 024101
- [23] 2003 *Inorganic Crystal Structure Database FIZ Karlsruhe, Germany* (Coverage: 1915–present) <http://www.stninternational.de/stndatabases/databases/icsd.html>
- [24] Gale J D 1997 *J. Chem. Soc. Faraday Trans.* **93** 629
- [25] Krivchikov A I, Gorodilov B Ya, Kolobov I G, Erenburg A I, Savvitskii D I, Ubizskii S B, Syvorotka I M and Vasylechko L O 2000 *Low Temp. Phys.* **26** 370

- [26] Anderson O L 1998 *Am. Mineral.* **83** 23
- [27] Schnelle W, Fischer R and Gmelin E 2001 *J. Phys. D: Appl. Phys.* **34** 846
- [28] Vočadlo L, Knight K S, Price G D and Wood I G 2002 *Phys. Chem. Miner.* **29** 132
- [29] Wood I G, Knight K S, Price G D and Stuart J A 2002 *J. Appl. Crystallogr.* **35** 291
- [30] Inaba H 1996 *Japan. J. Appl. Phys.* **35** 3522
Inaba H 1996 *Japan. J. Appl. Phys.* **35** 4730
- [31] Ruffa A R 1977 *Phys. Rev. B* **16** 2504
- [32] Zhao Y, Weidner D J, Parise J B and Cox D E 1993 *Phys. Earth Planet. Inter.* **76** 1